Manganese-Enhanced MRI reflects seizure outcome in a model for mesial temporal lobe epilepsy

S. Dedeurwaerdere, K. Fang, M. Chow, Y. Shen, I. Noordman, L. van Raay, N. Faggian, M. Porritt, G.F. Egan, T.J. O'Brien

PII: S1053-8119(12)01166-4
DOI: doi: 10.1016/j.neuroimage.2012.11.054
Reference: YNIMG 9990

To appear in: *NeuroImage*

Accepted date: 23 November 2012

Please cite this article as: Dedeurwaerdere, S., Fang, K., Chow, M., Shen, Y., Noordman, I., van Raay, L., Faggian, N., Porritt, M., Egan, G.F., O'Brien, T.J., Manganese-Enhanced MRI reflects seizure outcome in a model for mesial temporal lobe epilepsy, *NeuroImage* (2012), doi: 10.1016/j.neuroimage.2012.11.054

Manganese-Enhanced MRI reflects seizure outcome in a model for mesial temporal lobe epilepsy.

Dedeurwaerdere S[1, 2], Fang K[3], Chow M[2], Shen Y[2], Noordman I[2], van Raay L[2], Faggian N[3], Porritt M[2], Egan G.F.[3], and O'Brien TJ[2].

[1]Department of Translational Neuroscience, University of Antwerp, Wilrijk, Belgium

[2]Department of Medicine (RMH/WH), University of Melbourne, Parkville, VIC, Australia.

[3]Howard Florey Institute, University of Melbourne, Parkville, VIC, Australia.

Running title: MEMRI during *status epilepticus*-induced epileptogenesis

Author for correspondence: Stefanie Dedeurwaerdere

University of Antwerp

Department of Translational Neuroscience

FGEN CDE T4.20

University of Antwerp

Universiteitsplein 1

2610 Wilrijk, Belgium

TEL: +32 3 265 26 38

stefanie.dedeurwaerdere@ua.ac.be

Abstract

The neurobiological processes resulting in epilepsy, known as epileptogenesis, are incompletely understood. Manganese-enhanced MRI (MEMRI) can potentially aide in this quest as it provides superior tissue contrast, particularly of the hippocampal subregions. This longitudinal study aims to characterise the changes in the hippocampus of the post kainic acid-induced *status epilepticus* (KASE) rat model of mesial temporal lobe epilepsy using MEMRI *in vivo*.

Serial acquisition of T_1-weighted MEMRI images were taken before, 2 days and 6 weeks after KASE (10-30 mg/kg, i.p.) in 14 rats and in 11 control rats, while a second cohort of control (N= 6) and epileptic animals (N= 10) was imaged at 2 months post KASE only. $MnCl_2$ (50 mM, 10 µl) was administered in the right lateral ventricle 1 day before scanning. Regions of interest were drawn around the hippocampus and several subregions of the hippocampus (CA1, CA3 and dentate gyrus). Markers of epilepsy such as spontaneous recurrent seizures, hippocampal neuronal loss and mossy fiber sprouting were quantified.

A persistent increase in MEMRI signal intensity was found in the hippocampus, CA1 and dentate gyrus in the KASE group compared to the control group (ANOVA $p<0.05$). The intensity signal in the hippocampus and subregions correlated inversely with the frequency of spontaneous recurrent seizures in the chronic epileptic phase, however there was no relationship observed between histopathological changes such as cell loss and mossy fiber sprouting with seizures.

This study demonstrates that MEMRI is able to detect imaging changes in the hippocampus during the course of epileptogenesis relevant for seizure expression. These data strongly indicate a relationship between manganese enhancement and spontaneous seizure outcome, suggesting that MEMRI could provide a preclinical biomarker for the severity of epileptogenesis *in vivo* in animal models.

Key words: epileptogenesis, *status epilepticus*, neuroimaging, contrast agent, biological markers

Abbreviations:

EEG	electroencephalography
i.c.v.	intracerebroventricular
i.p.	intraperitoneal
KASE	kainic acid-induced *status epilepticus*
MEMRI	Manganese-enhanced magnetic resonance imaging
MRI	magnetic resonance imaging
CA	*cornus ammonis*

1. Introduction

Manganese was introduced almost two decades ago as a contrast enhancer for magnetic resonance imaging (MRI) and has since been applied in multiple areas of neuroscience research for revealing brain neuroarchitecture, cellular activity or malfunction and tract tracing of neuronal connections (Boretius and Frahm, 2011; Massaad and Pautler, 2011)(Van Meir and Van der Linden)(Koretsky and Silva, 2004). These applications of manganese enhanced MRI (MEMRI) take advantage of the following properties of the paramagnetic ion Mn^{2+}: it is a potent T_1-shortening agent and therefore regions with increased Mn^{2+} uptake are visualised as hyperintensities on T_1 weighted images; it is a calcium (Ca^{2+}) analogue that can enter neurons through voltage-gated Ca^{2+} channels; and once in the cells Mn^{2+} can be transported trans-synaptically along axons by microtubule-dependent axonal transport (Boretius and Frahm, 2011; Massaad and Pautler, 2011; Pautler et al., 1998). Of particular utility is its ability to clearly enhance the various subfields of the hippocampus, namely the granular layer of the dentate gyrus, and the pyramidal layer of *cornu ammonis (*CA) 1 and CA3.

Serial *in vivo* neuroimaging has the ability to non-invasively detect changes occurring during epileptogenesis, with the potential to provide novel insights into the basic pathophysiological mechanisms and to find and evaluate novel treatment strategies to prevent epilepsy (Grohn et al., 2011). Nairismagi et al. (2006) reported that manganese-enhanced T_1 MRI contrast is representative of mossy fibre sprouting in the hippocampus, a common pathologic finding in temporal lobe epilepsy, in the post kainic acid-induced status epilepticus (KASE) model. Increased manganese enhancement in chronic epileptic animals with mossy fiber sprouting was recently confirmed by Malheiros et al. (2012). In contrast, a second study found a decrease of manganese enhancement in hippocampal subregions at the early phase of epileptogenesis and a recovery of the enhancement in the latent and chronic phases (Alvestad et al., 2007). In a neuronal activation study with MEMRI, CA3 hyperintensity was found shortly after acute kainic acid administration (Hsu et al., 2007). Furthermore, a recent study by Immonen et al. (2008)

found abnormal MEMRI hyperintensity in the CA1 and the dentate gyrus at two months post-SE, but not at earlier time points. As an explanation for these seemingly contrasting results, we hypothesised that there may be a link between the MEMRI findings and the functional hallmark of epilepsy, namely the emergence of spontaneous recurrent seizures. This possibility had not been systematically investigated in the previous studies. To investigate this hypothesis we undertook a longitudinal study utilising serial MEMRI in the same animals. The study aimed to obtain a better understanding of the structural, morphometric and intensimetric changes on MEMRI that occur during epileptogenesis in the KASE model, and to determine the relationship of these changes to the occurrence of spontaneous seizures and histological accompaniments of epileptogenesis, namely hippocampal neuronal loss and mossy fiber sprouting.

2 Methods

2.1 Animals

Adult Wistar male in-bred non-epileptic control rats (N= 41, 200-250 g and 7-8 weeks of age) were used. The animals were singly housed in standard opaque plastic cages with food and water *ad libitum*. They were maintained on a 12 h light/dark cycle (lights on at 6 a.m.) at 22°C with 60% relative humidity and treated in accordance with the Australian NH&MRC Code of conduct for use of animals in research. The study protocol was approved by the Institutional Animal Ethics Committees of the University of Melbourne.

2.2 Study design

The study involved two cohorts of rats. In the first cohort, serial MEMRI T_1 weighted scans were acquired in the epileptic rat model pre- (N= 14), 2 days (N= 14) and 6 weeks post-KASE (N= 10) and in a matched control group (N= 11, N= 9 and N= 7, respectively). During the study, some animals needed to be excluded due to technical failures such as electrode cap dislocation. Animals were implanted with a MRI compatible intracerebroventricular (i.c.v.) guide cannula for $MnCl_2$ injection and MRI compatible epidural EEG electrodes to detect seizure activity. After one week of recovery, $MnCl_2$ was administered i.c.v. one day before each MRI scan. Continuous 24h video-electroencephalography (video-EEG) monitoring was performed to quantify the frequency of occurrence of spontaneous recurrent seizures at least twice between 4, 5 and 6 weeks post KASE. After the last video-EEG session, animals were sacrificed, perfused with preserving solution and the brains extracted for histological assessment.

In the second cohort of rats, KASE (N= 10) and control (N= 6) animals had their MEMRI scan acquired at the chronic epileptic stage only (> 2 months post KA) to endorse the findings of the final time point in the first study and to control for potential toxicity by repeated Mn^{2+} administration. In these animals, $MnCl_2$ was injected stereotaxically i.c.v. under general anaesthesia two months post saline or KASE injections with an MRI scan acquired the following

day. Within the next week, EEG electrodes were implanted and continuous video-EEG monitoring was performed for five days after one week of recovery to quantify the spontaneous recurrent seizures.

2.3 Implantation of i.c.v. guide cannula and EEG electrodes

In the serial MEMRI group (cohort 1), a plastic guide cannula (length= 5.5 mm, internal diameter= 0.39 mm, Plastics One, Canada) was implanted stereotaxically into the right lateral ventricle according to established procedures (Morris et al., 2007) to allow repeated $MnCl_2$ administration as well as with two epidural MRI compatible electrodes (Plastic ones, Canada) and two plastic or silver (Jewellery by JARC, Australia) anchoring screws (van Raay et al., 2009). Briefly, the tips of the Teflon coated platinum bipolar electrode were placed epidurally through small burr holes across the frontal cortex, while the anchoring screws were placed into the occipital bone. Dental cement was used to fix the bipolar electrode, the i.c.v. cannula and screws in place. Animals received an intraperitoneal (i.p.) injection of carprofen (0.5 mg/kg) (Pfizer Animal Health Group, Australia) for pain alleviation, 1 ml of saline to prevent dehydration and were placed on a heating mat (Thermofilm PET Heater, Thermofilm, Australia) for recovery. Proper placement of the cannula was evaluated by i.c.v. injection of 2 nmol (4 µl) angiotensin II (Auspep Pty, Melbourne, Australia), three days post-operatively and changes in the rat's water intake were assessed according to Morris et al. (2007). Based on the angiotensin II test, one animal was excluded.

In the second cohort, six epidural EEG electrodes were implanted according to Van Raay et al. (2009), while $MnCl_2$ was injected stereotaxically as described below.

2.4 Kainic acid-induced *status epilepticus* (KASE)

Status epilepticus was induced by i.p. injection of kainic acid in twenty-four male rats as described previously (Dedeurwaerdere et al., 2011; van Raay et al., 2009; Vivash et al., 2011).

Briefly, repeated i.p. injections of kainic acid (Oceans Produce Industries, Nova Scotia, Canada) (2.5-5 mg/kg) were given every 45-60 min until sustained seizure activity was induced for 4 h, while control rats (N= 17) received saline injections and comparable handling. After 4 h of *status epilepticus*, animals were given diazepam (4 mg/kg, i.p, Roche Products, NSW, Australia) to terminate the *status epilepticus*.

2. 5 MEMRI acquisitions

In the first cohort, the i.c.v. injections of $MnCl_2$ (50 mM, 10 µl) were administered one day prior to the MRI acquisitions in awake animals. Dosing and volume was based on previous studies, which allowed detection of cortical laminar architecture (Silva et al., 2008). One limitation to the use of Mn^{2+} as a contrast agent is its cellular toxicity (Bouilleret et al., 2011). Currently, there is no approved clinical application for manganese-enhanced brain imaging in humans. The use of i.c.v. injection in our study enables focal administration of Mn^{2+} to the brain without systemic exposure and hence reducing potential toxicity to peripheral organs such as the heart. The $MnCl_2$ was slowly infused over 5 min to prevent trauma to the brain from a sudden increase in ventricular pressure. A precision glass syringe was connected with Teflon tubing filled with distilled water and an air bubble spaced between the distilled water and $MnCl_2$ solution; movement of the air bubble indicated the flow of the $MnCl_2$ solution. The injection needle was left in place for another 10 min, to prevent backflow, before being removed and closure of the guide cannula with a plastic cap. Serial MEMRI scans were acquired in the control and KASE groups at three time points: (i) baseline, (ii) early epileptogenesis (2 days) and (iii) chronic phase (6 weeks).

In the second cohort, $MnCl_2$ (50 mM, 10 µl) was injected in the right lateral ventricle as above, however under ketamine/xylazine anaesthesia (75 mg/kg and 10 mg/kg, respectively, Lyppard, Australia) while fixed in the stereotaxic frame. Animals received i.p. injection of carprofen (0.5 mg/kg) (Pfizer Animal Health Group, NSW, Australia) for pain alleviation, and 1

ml of saline to prevent dehydration. Following the injection, the incision was sutured and animals were allowed to recover on a heating mat. In these animals, a single MEMRI scan was taken in the chronic epileptic phase (~2 months post KASE).

MRI scanning for both cohorts was acquired the day following the $MnCl_2$ injections on a 4.7 T Biospin (Bruker, Germany) under isoflurane anaesthesia (5% induction and 1-3% maintenance in medical air and oxygen). It has been shown previously that a 24-hour uptake period of $MnCl_2$ results in optimal signal enhancement (Boretius and Frahm, 2011). Rats were secured on an animal bed with a respiration sensor and the surface coil (customised with a hole to fit the bipolar electrode and guide cannula) was always placed in the same position around the implant on the head of the rat. A pilot scan was taken to ensure adequate coverage of the brain followed by the MRI T_1 acquisition which took 1h 13 min to complete. The MRI scanning protocol consisted of a 3D gradient recalled echo with TR= 15 ms, TE= 5 ms, flip angle= 25°, averages= 24, matrix= 256 x 92 x 64, FOV= 25 x 25 x 25 mm^3, resolution= 0.098 x 0.13 x 0.391 mm^3/voxel, interlaced.

2.6 MEMRI analysis:

Using the Analyze v 8.1 software (Mayo Clinic, USA) freehand Volumes of Interest (VOIs) were drawn around the hippocampus and CA1, CA3 and dentate gyrus subregions of the left brain hemisphere on consecutive axial MEMRI slices (Fig 1) using Graph Pen (WACOM, China), with the analyzer blinded to the animal's treatment group. The MEMRI scans were coregistered to a reference image and segmented to a voxel dimension of 0.098 x 0.098 x 0.39 mm. Given that brain abnormalities in the systemic induced KASE model are bilaterally uniform and to avoid volumetric and intensimetric bias due to the implantation of the guide cannula and $MnCl_2$ injection in the right lateral ventricle, only the left hemispheric measurements were taken into account. Volumetric measurements were analysed for the hippocampus, which was delineated based on the difference in contrast between the hippocampus and the corpus callosum,

ventricles and thalamus (Fig. 1). For the intensimetric changes, manganese enhancement was measured as the T_1 signal intensity in the dorsal hippocampus, CA1, CA3 and dentate gyrus subregions from bregma -2.64 till -4.56 mm (Paxinos and Watson, 2007)(Fig. 1). Intensity values for each region were normalised against the intensity of the brain hemisphere (delineated by the auto-trace tool of Analyze v8.1) covering the VOIs to account for differences between animals in overall manganese intensity due to variations in absorption of Mn^2 (Bouilleret et al., 2009). A cortical normalisation region (Fig. 1) was evaluated, but induced more noise compared to the brain hemisphere normalisation. Brain hemispheric T1 signal was not different between control and KASE group and was stable over time. Brain hemisphere normalisation resulted in robust and reproducible results with equivalent measures between control and KASE group at baseline. In the first longitudinal study cohort, volume and intensity values were expressed as percentage of baseline. For the second cohort, raw volume data and normalised intensities were presented.

An in-house written algorithm (by NF) based on MATLAB Software (MathWorks, USA) enabled the measurement of the thickness of the CA1. A straight perpendicular line was drawn between the boundary of the corpus callosum and the molecular layer of the dentate gyrus, which are both substantially lower in signal intensity. Approximately three sections for each scan were included in the analysis, blinded with respect to the treatment group. Only scans providing clear boundaries were included in the analysis.

2.7 Video-EEG monitoring

Video-EEG monitoring was performed in awake and freely moving control and KASE animals with food and water *ad libitum*. For the first cohort, a MacLab based system (Animal Bio Amp, Powerlab and Chart Software v1.5.3, AdInstruments, USA) was used for EEG recording. A separate digital video system focusing on the cages and a digital clock, was equipped with infrared lighting for night-time recordings (3–8 mm, Pentax, USA) and coupled to QuickTime

software (Apple, USA) for recording. In the second cohort, VEEGM was performed as described previously (van Raay et al., 2009).

Seizures were identified on the EEG traces by a reviewer blinded to treatment group, and confirmed by reviewing the accompanying video recording at the corresponding time point. Seizures were defined electrographically as oscillatory EEG patterns that contained spikes and waves, which evolved in frequency and amplitude. The amplitude had to be at least two times baseline and a minimum duration of > 5 s. All EEG abnormalities were reviewed by two independent reviewers to reach consensus about what to classify as a seizure.

2.8 Histology

At the end of the experimental period, animals were euthanized via injection of a lethal dose of anaesthetic (325 mg/rat pentobarbitone sodium, i.p., Virbac Animal Health, Carros Cedex, France) and transcardially perfused with 4% paraformaldehyde (ACROS Organics, USA) to allow histological assessment of the brains. Brains were dissected and post-fixed in 4% paraformaldehyde for two days followed by immersion in a 20% sucrose solution for 1-2 days. The brains were placed in a brain box filled with embedding medium (Tissue-Tek O.C.T., ProSciTech, Australia) and frozen in 2-methylbutane on liquid nitrogen before being stored in an -80°C freezer until processing.

Consecutive coronal brain sections (30 µm, bregma= -0.9 mm) were sliced in quadruplicate and thaw-mounted on 1% gelatinised Superfrost glass slides (Menzel-Glaser, Germany) for assessment of cell loss (Thionine stain) and mossy fiber sprouting (Timm's stain) (Liu et al., 2009; Vivash et al., 2011).

Stereological quantification with the optical fractionator method was used in a subgroup of KASE animals (N= 8) to quantify pyramidal neuronal numbers in CA1 utilising StereoInvestigator Software (MBF Bioscience, USA) (Vivash et al., 2011; West et al., 1991). Counting was performed on one in every fifth section collected between bregma -2.64 mm and -

4.56 mm (Paxinos and Watson, 2007) to include the dorsal CA1 region. Regions of interest were first delineated at 20x magnification (Olympus Uplan Apo lens, USA) while actual counts were performed at 100x magnification (oil immersion Olympus Uplan Apo lens, USA). Estimates of CA1 pyramidal neurons were determined using an unbiased counting frame of dimension 25 µm (width-x) x 25 µm (length-y) x 10 µm (height-z). These counting frames were assigned to the region of interest according to the location of intersections on a grid. The grid had a dimension 200 x 200 μm^2 and was randomly placed over the ROI. Grid and counting frame size were chosen to ensure a suitable number of cells were sampled (minimum 200) to compensate for inter-section variability and to reduce error.

A visual scale method was used to quantify cell loss in CA1 (and validated with stereological counting, see results), CA3 and dentate hilus in control and KASE animals. Pictures were taken of 6-8 coronal brain section between bregma -2.64 mm and -4.56 mm at a 4x (Leitz Wetzler lens, Germany) magnification using a Nikon microscope (Japan) of 14 controls and 14 KASE treated animals. All pictures were blinded with respect to treatment. Two independent observers scored the regions using five levels (from 0 to 4) of neuronal loss. These levels were 0: no stained neurons, 1: very sparse stained neurons, 2: some stained neurons, 3: many neurons with slightly disturbed cell layer integrity and 4: many stained neurons with normal cell layer integrity.

Mossy fiber sprouting was assessed blinded in at least eight Timm's stained coronal brain sections (from bregma -2.64 to -4.56 mm) of the hippocampus of control (N= 12) and KASE (N= 15) animals as previously described (Liu et al., 2009; Vivash et al., 2011). For this, the optical density (OD) was measured in the stratum moleculare of the dentate gyrus and normalised against the OD of the stratum radiatum according.

2.9 Statistical analysis

Statistical analysis was performed using Prism 5 for Mac OS X v5.0d (GraphPad Software, USA). For the longitudinal data a two-way ANOVA was used with post-hoc Bonferroni testing to

evaluate group differences at the different time points. Volume changes between control and KASE group were analysed using Student's t-test. Visual cell number scale data were compared between groups using the non-parametric Mann Whitney U test. Mossy fiber sprouting quantification was compared between control and KASE groups using Student's t-test. Correlations between parameters were tested using the Spearman rank correlation coefficient ρ. Statistical significance was set at $P<0.05$. P-levels of >0.05-0.1 were mentioned to indicate trends or borderline significant differences. Data were expressed as mean ± standard error of the mean (SEM) except for cell loss data derived from the visual scale, which were presented as median with interquartile ranges and minimum and maximum (box plot).

3 Results

3.1 Hippocampal volumetric measurements in the KASE model

There was no significant difference in hippocampal volume between the control and KASE groups, nor any change over time in the longitudinal study (Fig. 2A). However, at the chronic stage, two animals displayed hippocampal shrinkage and enlarged ventricles (Fig. 2B). These animals also displayed marked hippocampal pyramidal neuronal loss on histological examination.

3.2 Hippocampal CA1 subregion thickness on MEMRI in the KASE model

The enhanced tissue contrast afforded by the use of $MnCl_2$ enabled the measurement of the thickness of the CA1 subregion of the hippocampus on the MRI images. CA1 thickness was significantly lower in the KASE group compared to the control group at both the early and chronic epileptic time point post *status epilepticus*, but did not significantly progress between the two time points (Fig. 3). Post-hoc testing showed a significant difference at the chronic phase only ($P< 0.05$), although the magnitude of the decrease was similar at the early time point.

3.4 Longitudinal changes in manganese signal enhancement in the hippocampus in the KASE model

The T_1 signal intensity in the DG and the CA1 hippocampal subregions were significantly greater in the two post-KASE scans (relative to the baseline scan), compared to the control group ($P< 0.05$) (Fig. 4). For the hippocampus as a whole there was a trend for a significant increase in the KASE group ($P= 0.069$). In CA3, there was no significant difference between control and KASE treated animals.

3.5 Spontaneous epileptic seizures

Spontaneous seizures were recorded in 15/20 (75%) of KASE at least 6 weeks following the SE, with the average seizure frequency in individual animals ranging from <1 to 5 seizures per day. There was a trend ($P= 0.081$) for an inverse correlation between MEMRI signal intensity in the dentate gyrus two days after the KASE and future seizure expression at 6 weeks post SE (Fig. 5A). At six weeks post SE, the MEMRI signal intensity in all regions investigated showed a significant inverse correlation with seizure expression (Fig. 5B). These results were reinforced by the data from the second cohort of animals which were scanned at the chronic phase only (Fig. 5C), indicating that animals with more seizures had lower MEMRI signal compared to KASE animals with no or limited seizures.

3.6 Histopathological changes in the chronic epileptic phase in the KASE model

3.6.1 Hippocampal neuronal loss

A blinded visual cell rating scale was used to assess the degree of neuronal loss in subregions of the hippocampus. This method was validated in a subset of animals ($n= 9$) by comparing the visual cell rating scale in the CA1 region of the hippocampus with the golden standard method of stereological counting west (West et al., 1991). This showed a strong correlation between the results obtained with both methods ($\rho= 0.71$) (Fig. 6). Significant neuronal loss was observed in

all regions investigated, namely CA1 (P< 0.01), CA3 (P< 0.01), CA4 (P< 0.001) and dentate hilus (P< 0.001) (Fig. 6).

Even though significant cell loss was observed in CA1 in the KASE group, no direct relationship was found between cell loss and CA1 thickness.

A significant correlation was found between the degree of neuronal cell loss and the MEMRI intensity in the corresponding brain area for CA1 (P< 0.05), while for CA3 this was close to significance (P= 0.056) (Fig. 7).

There was no correlation between the severity of neuronal cell loss for any of the hippocampal regions and the average number of seizures per day recorded in the chronic epileptic phase.

3.6.2 Hippocampal mossy fiber sprouting

There was a significant difference in ROD of the stratum moleculare of the dentate gyrus between control and KASE group (P< 0.001) on the Timm's stained sections from animals sacrificed at the chronic epileptic phase, indicating mossy fiber sprouting (Fig. 8).

There was no significant correlation between the degree of mossy fiber sprouting and the MEMRI signal intensity in dentate gyrus.

There was also no significant correlation in the intensity of the mossy fiber sprouting and the average number of spontaneous seizures per day recorded. There was also no significant relationship between the severity of the cell loss in the CA3 or dentate hilus subregions and the intensity of the mossy fiber sprouting.

4. Discussion

In this study we used the high contrast MEMRI technique to serially assess for volumetric, morphometric and intensimetric changes in subregions of the hippocampus *in vivo* during epileptogenesis in the KASE rat model of mesial temporal lobe epilepsy. Using this technique we demonstrated differences in Mn^{2+} enhancement in the dentate gyrus and CA1 region of KASE animals, compared to control animals, that was present early following the SE and persisted into the chronic epileptic stage. While no relationship was found between histopathological changes such as cell loss and mossy fiber sprouting with seizures, the intensity signal in the hippocampus and subregions correlated inversely with seizure expression at the chronic epileptic phase. Most interestingly, two days post KASE a borderline significant inverse correlation was found between dentate gyrus intensity and future seizure expression. These data strongly indicate for the first time a relationship between manganese enhancement and spontaneous seizure expression, suggesting that MEMRI could act as a biomarker for the severity of epileptogenesis.

There was no significant change in the overall volume of the hippocampus, indicating lack of significant macroscopic hippocampal atrophy. In a previous study by our group, we had similar results in the KASE model using this inbred strain of Wistar rats (unpublished data). Strain differences may play a role in the extent of hippocampal sclerosis after *status epilepticus* as previous studies have shown distinct differences in neurodegeneration not only between strains, but also between animal model vendors (Langer et al., 2011; Portelli et al., 2009). However, in this study the use of MEMRI allowed the measurement of the width of the CA1 sub-hippocampal region *in vivo* that demonstrated a reduction in the KASE animals compared to controls.

A key finding of our study was that the MEMRI intensity in several hippocampal subregions correlated inversely with seizure expression at six weeks post KASE, that was confirmed when increasing the study population with a second cohort (N= 20 in total). This suggests that Mn^{2+} uptake in the hippocampus is a functional biomarker of seizure burden. Given that seizure susceptibility varies from strain to strain and between rats from different vendors, this could

potentially explain the conflicting reports of change in MEMRI intensity from different studies in the KASE rat models (Alvestad et al., 2007; Immonen et al., 2008; Nairismagi et al., 2006). While the Finnish group found MEMRI hyperintensity in hippocampal subregions at a two months time point post KASE, Alvestad and colleagues found a pronounced decrease in MEMRI intensity early on (possibly as a consequence of the status epilepticus) and a normalization of MEMRI intensity at later time points. Additional factors that may contribute to these discrepancies are differences in the mode of $MnCl_2$ administration (subcutaneously versus intraperitoneally versus intracerebroventricularly), small group sizes and image analysis.

Narismägi et al. (2006) proposed that MEMRI reflects mossy fiber sprouting, which could explain the increase in MEMRI intensity in the DG and CA3. This is a plausible contributor to the MEMRI signal as the anatomical staining pattern revealed by Timm's (zinc) stain to analyse mossy fiber sprouting (zinc containing boutons) is very similar to that of the manganese enhancement pattern. Zinc is a bivalent anion like manganese, and therefore could replace calcium in the same manner as manganese in the brain. However, although significant mossy fiber sprouting was present in our cohorts of animals, we did not find a relationship between the mossy fiber sprouting data and MEMRI intensity. It is possible that the increased MEMRI signal intensity due to mossy fiber sprouting may be counterbalanced by other factors such as cell loss. Indeed, we found significant cell loss in CA1, CA3, CA4 and dentate hilus in the KASE animals. Also, a significant correlation was found between the magnitude of cell loss in CA1 and CA3 (trend) with the respective MEMRI intensity. This would indicate that MEMRI at least partly reflects the number of neurons present in the brain regions. Alvestad et al. (2007) and Hsu et al. (2007) made similar made to explain manganese intensity change in CA1.

We found that the histological hallmarks of limbic epileptogenesis, mossy fiber sprouting and neuronal loss in the hippocampus, did not correlate with the frequency of spontaneous seizures in our animals. This is consistent with the view that these changes occur early as a consequence of

the *status epilepticus* rather than due to the spontaneous recurrent seizures (Gorter et al., 2003; Pitkanen et al., 2002; Vivash et al., 2011).

The mechanisms underlying the inverse relationship between seizure expression and MEMRI intensity are uncertain. This intriguing association likely reflects a complex interplay between the contrasting effects of neuronal degeneration, neuronal sprouting/plasticity changes and neuronal excitation/suppression (Figure 9). Evidence exists that each of these individual mechanisms influence the MEMRI signal. Our results, and those of previous studies, indicate a correlation between cell loss and decreased MEMRI uptake (Natt et al., 2003). Brain inflammation occurs as a response to acute brain damage in this model (Dedeurwaerdere et al., In Press). Although astroglia have been thought to act as a metal sink in the brain and Kawai et al. (Kawai et al., 2010) has shown a correspondence between manganese-enhancement and astrogliosis in a focal ischemia model, Immonen et al. (2008) ruled out the contribution of astrogliosis and microgliosis as primary source of the MEMRI signal in the KASE model after careful histological comparison. We hypothesize that functional changes in cells or synaptic reorganisation are more likely to contribute to this finding than structural changes alone. Indeed also plasticity changes, including mossy fiber sprouting increase the MEMRI signal (Malheiros et al., 2012; Nairismagi et al., 2006). Finally, a relationship between neuronal activity and MEMRI signal has been well established (Boretius and Frahm, 2011; Hsu et al., 2007; Koretsky and Silva, 2004). Mn^{2+} has the capacity to substitute for Ca^{2+} in excitable tissues and is therefore thought to represent neuronal activity (Hsu et al., 2007). In rats with a relatively mild seizure frequency we observed more intense MEMRI intensity than in rats that were seizing more frequently. This inverse correlation was found in all subregions of the hippocampus. This apparent paradoxical result may be explained by secondary compensatory changes in the brain in frequently seizing rats. The increased intensity in low seizing rats could represent the expected hyperexcitability seen in TLE with increased Ca^{2+} influx (Cavazos and Cross, 2006). In contrast, in more frequently seizing rats a normalization of the manganese enhancement is seen. This may reflect decreased neuronal

activity in animals with more recurrent seizures as a protective mechanism of the brain against neuronal hyperexcitability. A recent study by our group demonstrated decreased neuronal metabolic activity during early epileptogenesis *in vivo* using serial ^{18}F-FDG PET imaging in the same animal model, with the hypometabolism becoming more marked after the onset of spontaneous recurrent seizures (Jupp et al., 2012). Such interictal hypometabolic changes in the hippocampus of patients with medically refractory TLE are well established with FDG PET (Goffin et al., 2008). We postulate based on our novel findings and previous studies that the final manganese enhancement of the T1 signal is the sum of neuronal cell density and the physiological processes involved in plasticity and neuronal activity.

Overall as a group, we found increased MEMRI intensity in the KASE group compared to controls. Although not statistically significant, the MEMRI intensity trended towards a reduction over time in the control group compared to the baseline condition, while in the KASE group there was a slight non-significant increase over time. This could reflect changes in the brain secondary to the indwelling catheter and the repeated injections such as a decrease in neuronal activity in the hippocampus of the control rats as they aged, as well as technical factors associated with the diffusion of the i.c.v administered Mn^{2+} from the ventricles. However, these factors would have affected the control and the post-KA SE rats equivalently. Thus we do not believe that this apparent longitudinal reduction in control MEMRI intensity affects our key finding of an inverse relationship between seizures and MEMRI signal. Furthermore, this result was confirmed by the second experiment in which the control and epileptic groups were imaged only once in the chronic phase to control for potential Mn^{2+} toxicity due to repeated administration.

Due to the currently unresolved toxicity of acute manganese injections, our findings will not readily find applications in patients. The key contribution of this study lies in providing an important link to understand the seemingly contradicting MEMRI results in epilepsy models in the past by demonstrating a close-relationship with seizure expression rather than histological data, which supports MEMRI as a comprehensive preclinical biomarker for studying

epileptogenesis. The dichotomy between low-seizing and high-seizing animals gives great opportunities for evaluating prophylactic curative treatments in conjunction with video-EEG recording. Video-EEG monitoring will identify treatments that were not effective, however, differentiating between low seizing animals and cured animals is much more challenging. Video-EEG monitoring is often limited to days or to a couple of weeks due to practical reasons (monitoring capacity and data handling). MEMRI in combination with video-EEG monitoring may give for the first time the possibility to distinguish animals with a low seizure outcome (high MEMRI signal) from truly 'cured' animals through different measurable parameters (baseline levels of MEMRI signal, no alterations in CA1 thickness or hippocampal volume). If the relationship that we have demonstrated with seizure activity is confirmed by other groups, then this could be used as an in-vivo imaging biomarker for proof of concept interventions aimed at mitigating epileptogenesis.

Acknowledgement

We would like to acknowledge the help of Rink-Jan Lohman for setup of the MacLab video-EEG monitoring system and Sian Price for assisting with seizure quantification.

This work was supported by an Early Career Research Grant from the University of Melbourne to Stefanie Dedeurwaerdere, BOF University of Antwerp and FWO.

References:

Alvestad, S., Goa, P.E., Qu, H., Risa, O., Brekken, C., Sonnewald, U., Haraldseth, O., Hammer, J., Ottersen, O.P., Haberg, A., 2007. In vivo mapping of temporospatial changes in manganese enhancement in rat brain during epileptogenesis. Neuroimage 38, 57-66.

Boretius, S., Frahm, J., 2011. Manganese-enhanced magnetic resonance imaging. Methods Mol Biol 771, 531-568.

Bouilleret, V., Cardamone, L., Liu, C., Koe, A.S., Fang, K., Williams, J.P., Myers, D.E., O'Brien, T.J., Jones, N.C., 2011. Confounding neurodegenerative effects of manganese for in vivo MR imaging in rat models of brain insults. J Magn Reson Imaging 34, 774-784.

Bouilleret, V., Cardamone, L., Liu, Y.R., Fang, K., Myers, D.E., O'Brien, T.J., 2009. Progressive brain changes on serial manganese-enhanced MRI following traumatic brain injury in the rat. J Neurotrauma 26, 1999-2013.

Cavazos, J.E., Cross, D.J., 2006. The role of synaptic reorganization in mesial temporal lobe epilepsy. Epilepsy Behav 8, 483-493.

Dedeurwaerdere, S., Callaghan, P., Pham, T., Rahardjo, G.L., Amhaoul, H., Berghofer, P., Quinlivan, M., Mattner, F., Loc'h, C., Katsifis, A., Grégroire, M., In Press. PET imaging of brain inflammation during early epileptogenesis in a rat model of temporal lobe epilepsy. Eur J Nucl Med Mol Imaging.

Dedeurwaerdere, S., van Raay, L., Morris, M.J., Reed, R.C., Hogan, R.E., O'Brien, T.J., 2011. Fluctuating and constant valproate administration gives equivalent seizure control in rats with genetic and acquired epilepsy. Seizure 20, 72-79.

Goffin, K., Dedeurwaerdere, S., Van Laere, K., Van Paesschen, W., 2008. Neuronuclear assessment of patients with epilepsy. Semin Nucl Med 38, 227-239.

Gorter, J.A., Goncalves Pereira, P.M., van Vliet, E.A., Aronica, E., Lopes da Silva, F.H., Lucassen, P.J., 2003. Neuronal cell death in a rat model for mesial temporal lobe epilepsy is

induced by the initial status epilepticus and not by later repeated spontaneous seizures. Epilepsia 44, 647-658.

Grohn, O., Sierra, A., Immonen, R., Laitinen, T., Lehtimaki, K., Airaksinen, A., Hayward, N., Nairismagi, J., Lehto, L., Pitkanen, A., 2011. Multimodal MRI assessment of damage and plasticity caused by status epilepticus in the rat brain. Epilepsia 52 Suppl 8, 57-60.

Hsu, Y.H., Lee, W.T., Chang, C., 2007. Multiparametric MRI evaluation of kainic acid-induced neuronal activation in rat hippocampus. Brain 130, 3124-3134.

Immonen, R.J., Kharatishvili, I., Sierra, A., Einula, C., Pitkanen, A., Grohn, O.H., 2008. Manganese enhanced MRI detects mossy fiber sprouting rather than neurodegeneration, gliosis or seizure-activity in the epileptic rat hippocampus. Neuroimage 40, 1718-1730.

Jupp, B., Williams, J., Binns, D., Hicks, R.J., Cardamone, L., Jones, N., Rees, S., O'Brien, T.J., 2012. Hypometabolism precedes limbic atrophy and spontaneous recurrent seizures in a rat model of TLE. Epilepsia 53, 1233-1244.

Kawai, Y., Aoki, I., Umeda, M., Higuchi, T., Kershaw, J., Higuchi, M., Silva, A.C., Tanaka, C., 2010. In vivo visualization of reactive gliosis using manganese-enhanced magnetic resonance imaging. Neuroimage 49, 3122-3131.

Koretsky, A.P., Silva, A.C., 2004. Manganese-enhanced magnetic resonance imaging (MEMRI). NMR Biomed 17, 527-531.

Langer, M., Brandt, C., Loscher, W., 2011. Marked strain and substrain differences in induction of status epilepticus and subsequent development of neurodegeneration, epilepsy, and behavioral alterations in rats strain and substrain differences in an epilepsy model in rats. Epilepsy Res 96, 207-224.

Liu, D.S., O'Brien, T.J., Williams, D.A., Hicks, R.J., Myers, D.E., 2009. Lamina-specific changes in hippocampal GABA(A)/cBZR and mossy fibre sprouting during and following amygdala kindling in the rat. Neurobiol Dis 35, 337-347.

Malheiros, J.M., Polli, R.S., Paiva, F.F., Longo, B.M., Mello, L.E., Silva, A.C., Tannus, A., Covolan, L., 2012. Manganese-enhanced magnetic resonance imaging detects mossy fiber sprouting in the pilocarpine model of epilepsy. Epilepsia 53, 1225-1232.

Massaad, C.A., Pautler, R.G., 2011. Manganese-enhanced magnetic resonance imaging (MEMRI). Methods Mol Biol 711, 145-174.

Morris, M.J., Gannan, E., Stroud, L.M., Beck-Sickinger, A.G., O'Brien, T.J., 2007. Neuropeptide Y suppresses absence seizures in a genetic rat model primarily through effects on Y receptors. Eur J Neurosci 25, 1136-1143.

Nairismagi, J., Pitkanen, A., Narkilahti, S., Huttunen, J., Kauppinen, R.A., Grohn, O.H., 2006. Manganese-enhanced magnetic resonance imaging of mossy fiber plasticity in vivo. Neuroimage 30, 130-135.

Natt, O., Watanabe, T., Boretius, S., Frahm, J., Michaelis, T., 2003. Magnetization transfer MRI of mouse brain reveals areas of high neural density. Magn Reson Imaging 21, 1113-1120.

Pautler, R.G., Silva, A.C., Koretsky, A.P., 1998. In vivo neuronal tract tracing using manganese-enhanced magnetic resonance imaging. Magn Reson Med 40, 740-748.

Paxinos, G., Watson, C., 2007. The rat brain in stereotaxic coordinates, Sixth edition ed. Academic Press, London.

Pitkanen, A., Nissinen, J., Nairismagi, J., Lukasiuk, K., Grohn, O.H., Miettinen, R., Kauppinen, R., 2002. Progression of neuronal damage after status epilepticus and during spontaneous seizures in a rat model of temporal lobe epilepsy. Prog Brain Res 135, 67-83.

Portelli, J., Aourz, N., De Bundel, D., Meurs, A., Smolders, I., Michotte, Y., Clinckers, R., 2009. Intrastrain differences in seizure susceptibility, pharmacological response and basal neurochemistry of Wistar rats. Epilepsy Res 87, 234-246.

Silva, A.C., Lee, J.H., Wu, C.W., Tucciarone, J., Pelled, G., Aoki, I., Koretsky, A.P., 2008. Detection of cortical laminar architecture using manganese-enhanced MRI. J Neurosci Methods 167, 246-257.

van Raay, L., Morris, M.J., Reed, R.C., O'Brien, T.J., Dedeurwaerdere, S., 2009. A novel system allowing long-term simultaneous video-electroencephalography recording, drug infusion and blood sampling in rats. J Neurosci Methods 179, 184-190.

Vivash, L., Tostevin, A., Liu, D.S., Dalic, L., Dedeurwaerdere, S., Hicks, R.J., Williams, D.A., Myers, D.E., O'Brien, T.J., 2011. Changes in hippocampal GABAA/cBZR density during limbic epileptogenesis: relationship to cell loss and mossy fibre sprouting. Neurobiol Dis 41, 227-236.

West, M.J., Slomianka, L., Gundersen, H.J., 1991. Unbiased stereological estimation of the total number of neurons in thesubdivisions of the rat hippocampus using the optical fractionator. Anat Rec 231, 482-497.

Figures:

Fig. 1: MEMRI image with regions of interest contours delineated with ANALYZE. Green, left brain hemisphere; red, left cortex; yellow, left hippocampus; turquoise, left CA1; pink, left CA3 and blue, left dentate gyrus. Abbreviations: L, left.

Fig. 2: Volume measurements of the hippocampus. A) Serial measurements expressed as % of baseline (cohort 1) and B) chronic phase data (cohort 1 & 2) is expressed as volume (mm^3) in control and KASE animals. Note indicated by open squares, two animals with lower hippocampal volume. Data are presented as mean ± SEM.

Fig. 3: Measurement of CA1 thickness (mm^2) during epileptogenesis in control and KASE animals. The first two time points are only measured in cohort 1 while the chronic phase was measured in cohort 1 & 2. * indicates $P< 0.05$ compared to control. Data are presented as mean ± SEM.

Fig. 4: Longitudinal MEMRI intensity changes in hippocampus and subregions during epileptogenesis in control and KASE animals (cohort 1). Abbreviations: HC, hippocampus; DG, dentate gyrus. Data are expressed as % of baseline and is presented as mean ± SEM. * indicates $P< 0.05$ compared to control.

Fig. 5: Correlation of MEMRI intensity and seizure frequency. A) Borderline significant inverse correlation between MEMRI intensity in dentate gyrus (DG) at 48 h and number of seizures/day (cohort 1). B) Significant inverse correlation between MEMRI intensity in hippocampus (HC), dentate gyrus (DG), CA3 and CA1 at 6 weeks and number of seizures/day (cohort 1). C) Representative images showing increased MEMRI intensity (arrows) in hippocampal regions in

low-seizing animals compared to controls and high-seizing animals (cohort 2). Data are expressed as % of baseline and is presented as mean ± SEM. * indicates P< 0.05 and ** is P< 0.01.

Fig. 6: Thionine cell staining of the hippocampus in a representative control (A) and KASE (B) rat. The results from the visual cell number scale correspond with stereological cell counting of CA1. Significant cell loss was observed in CA1, CA3, CA4 and dentate hilus (DH). Arrows indicate cell loss. Abbreviations: #, number. ** indicates P< 0.01 and *** is P< 0.001 compared to control. Data are expressed as a box plot with median, 25^{th} and 75^{th} percentile and minimum and maximum values.

Fig. 7: Correlation between MEMRI intensity in hippocampal subregions CA1 and CA3 with the visual cell number scale. * indicates P< 0.05.

Fig. 8: Mossy fiber sprouting in the *stratum moleculare* of the dentate gyrus in KASE animals. Data are presented as the mean ratio of the relative optical density (ROD) of the *stratum moleculare* (SM) over the *stratum radiatum* (SR) ± SEM. *** indicates P< 0.001 compared to control.

Fig. 9: Hypothesis on the biological mechanisms giving rise to the manganese induced T_1 changes. An inverse relationship between seizures and Manganese-enhanced MRI signal was demonstrated and is hypothesised to reflect a complex interplay between neurodegeneration, plasticity changes and brain excitation.

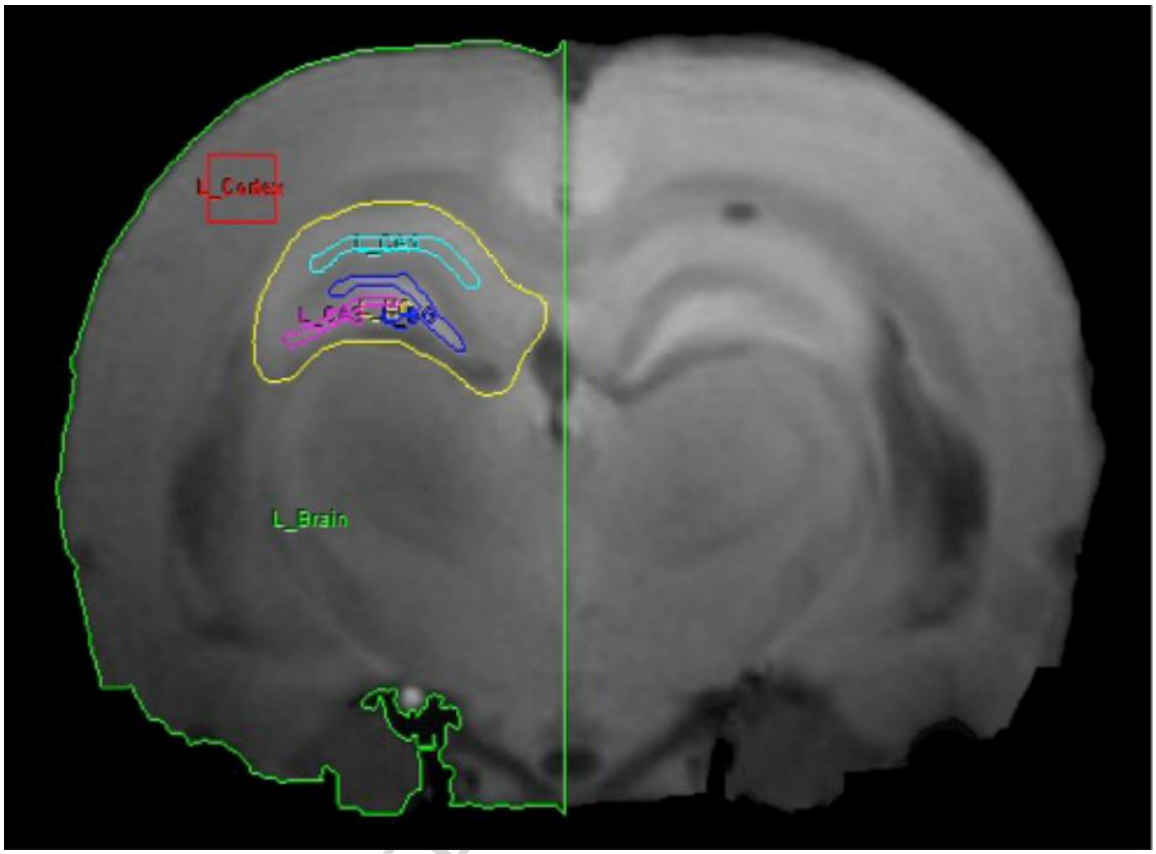

Figure 1

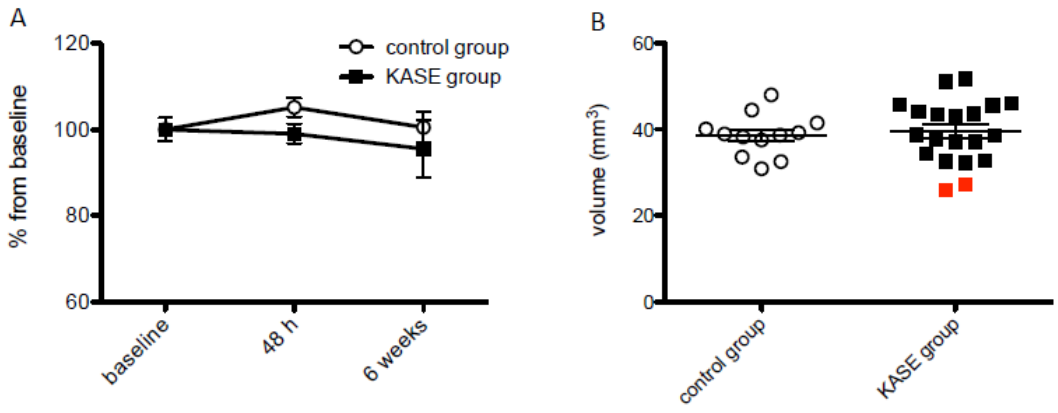

Figure 2

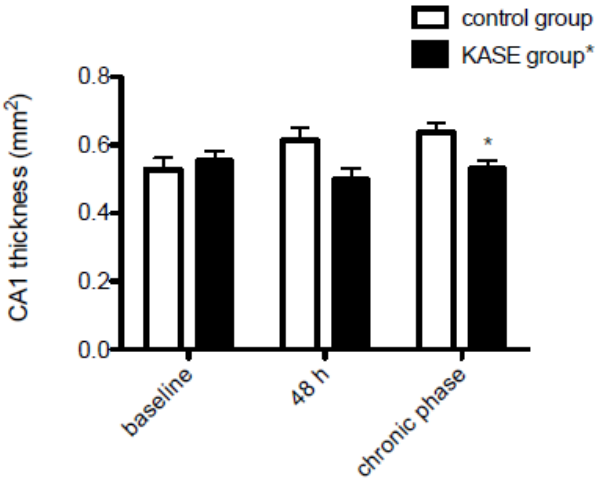

Figure 3

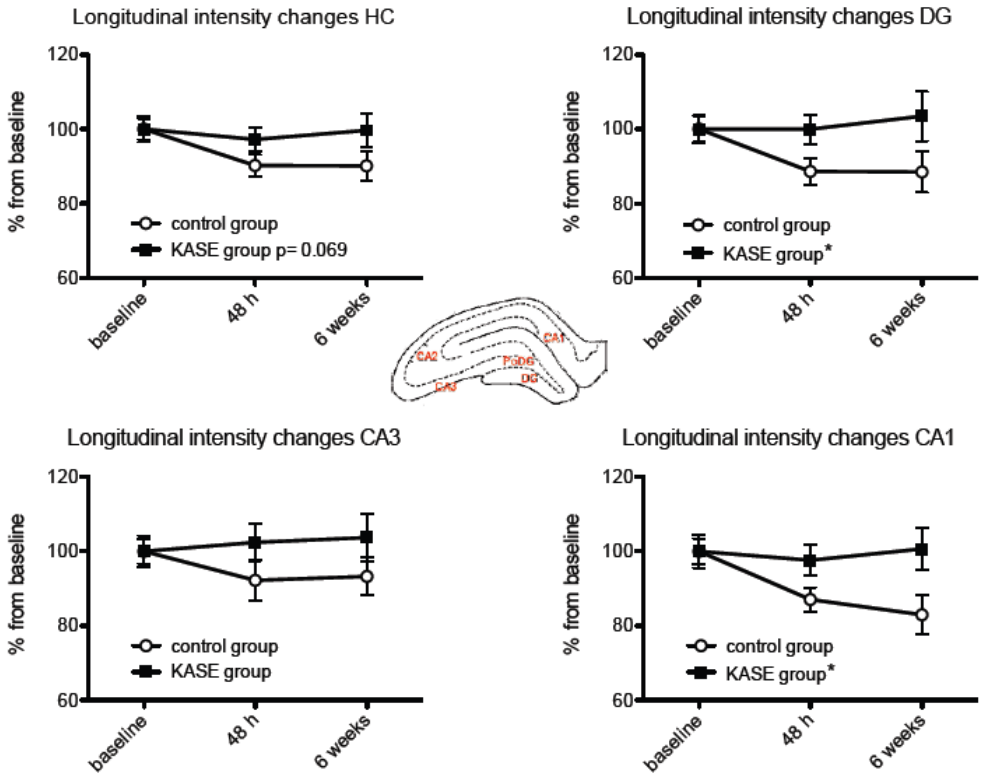

Figure 4

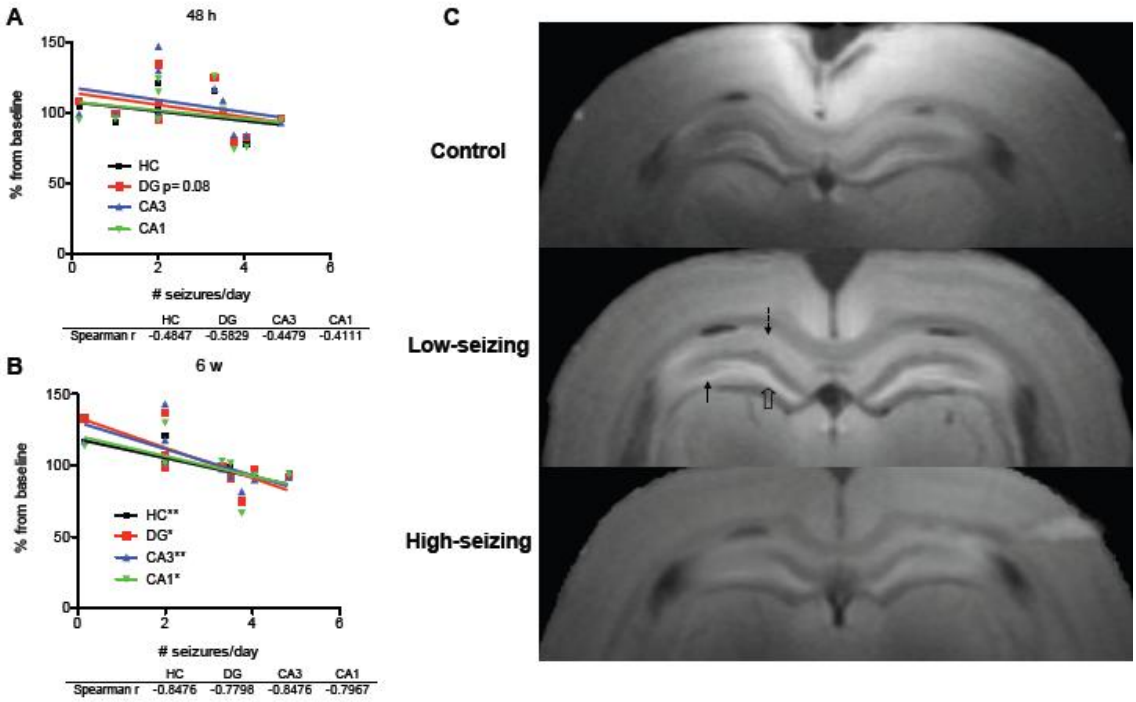

Figure 5

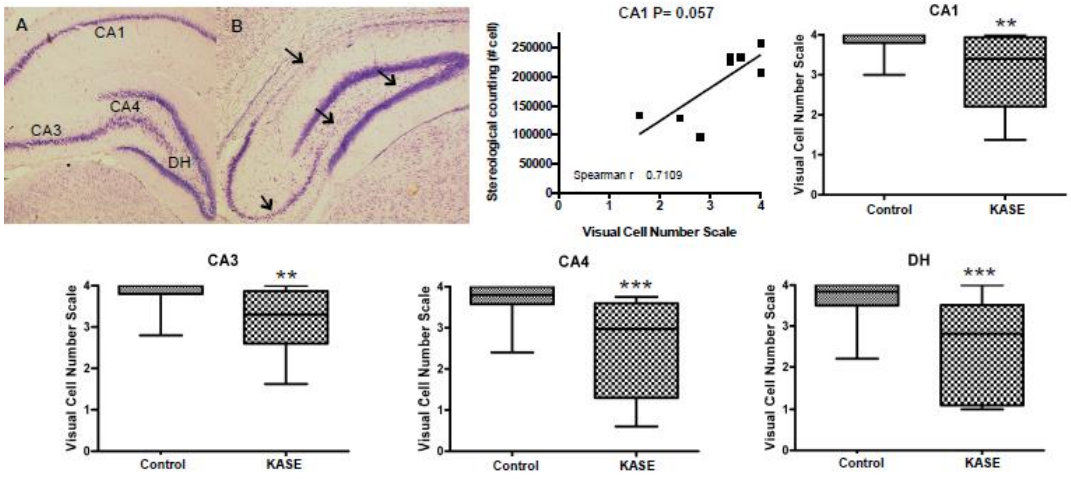

Figure 6

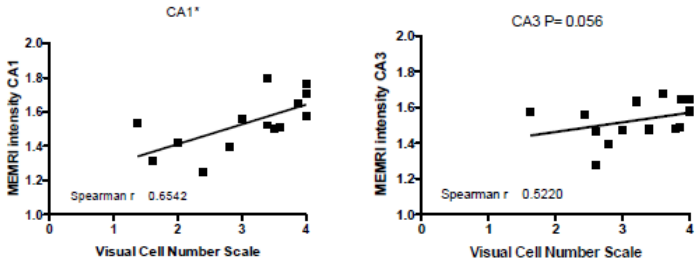

Figure 7

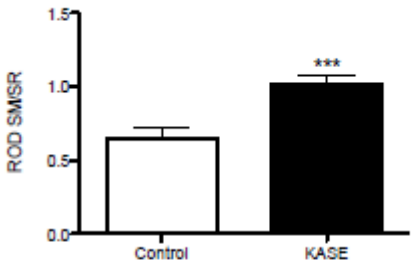

Figure 8

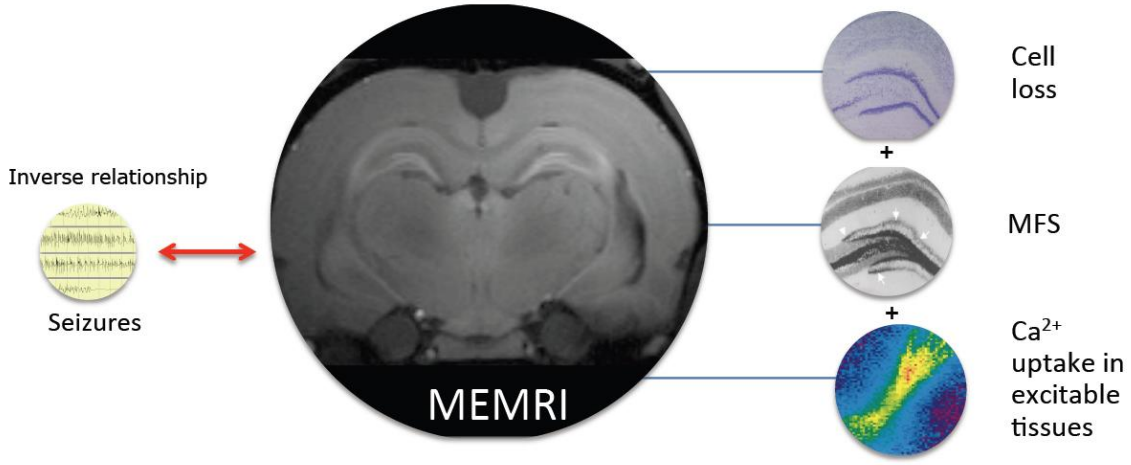

Figure 9

Highlights

High contrast MEMRI reveals persistent changes during epileptogenesis in the rat.

Manganese-enhancement in the dentate gyrus and CA1 region.

Complex inverse relationship between MEMRI intensity and seizure expression.

No relationship between histopathological changes and seizure expression.

MEMRI as a preclinical biomarker for evaluating disease-modifying treatments.

Author/s:
Dedeurwaerdere, S; Fang, K; Chow, M; Shen, Y-T; Noordman, I; van Raay, L; Faggian, N; Porritt, M; Egan, GF; O'Brien, TJ

Title:
Manganese-enhanced MRI reflects seizure outcome in a model for mesial temporal lobe epilepsy

Date:
2013-03-01

Citation:
Dedeurwaerdere, S., Fang, K., Chow, M., Shen, Y. -T., Noordman, I., van Raay, L., Faggian, N., Porritt, M., Egan, G. F. & O'Brien, T. J. (2013). Manganese-enhanced MRI reflects seizure outcome in a model for mesial temporal lobe epilepsy. NEUROIMAGE, 68, pp.30-38. https://doi.org/10.1016/j.neuroimage.2012.11.054.